| Sborník geologických věd | Užitá geofyzika 25 | Pages 117–143 | 33 figs. | 1 tab. | – pl. | Praha 1992<br>ISBN 80-7075-110-X<br>ISSN 0036-5319 |
|---|---|---|---|---|---|---|


# Detection of horizontal sheets by electromagnetic conductometers

## Detekovatelnost horizontálních deskovitých těles pomocí elektromagnetických konduktometrů


Richard Záhora[1]



Received April 11, 1990

*1 : 50,000*
*24 - 32, 24 - 33*
*25 - 13, 25 - 33*

*Electromagnetic prospection*
*Conductivity*
*Archaeological application*

Záhora, R. (1992): Detection of horizontal sheets by electromagnetic conductometers. – Sbor. geol. Věd, užitá Geofyz., 25, 117–143. Praha.



Abstract: The electromagnetic method with small induction number is applied to direct and contactless measurement of apparent conductivity of magnetic dipoles in a near field. The detection of sufficiently large horizontal conducting and non-conducting sheets with vertical and horizontal magnetic dipoles is explained and the detectability curves are drawn. Detectability of small-size inhomogeneities is discussed and estimated. The method has been applied in archaeological prospection.



[1]*Geofyzika,a. s., Brno, Ječná 29a, 612 46 Brno*


## Introduction

The direct contactless measurement of rock resistivities is based on the dependences of the measured components of electromagnetic field on apparent resistivity of an equivalent conducting half-space. These dependences are much more simple if the induction number $N = r/\delta$ is small (or if there is a near zone), i.e. the skin depth $\delta$ is much greater than the transmitter-receiver separation and than the thickness of a horizontally layered half-space, i.e.

$$N = \frac{r}{\delta} << 1\,, \quad \frac{h_i}{\delta} << 1 \tag{1}$$

where $\delta = \sqrt{2/\omega\mu\sigma}$ is the depth of skin.

## Direct contactless measurement of apparent conductivity

Let us consider a vertical transmitter-receiver magnetic dipole array located on the surface of a horizontally layered conducting half-space, as it is illustrated in Fig. 1. The conductivity of the layers is $\sigma_i$ and their thickness is $h_i$. Let us assume that the condition of a small induction number given by equations (1) is satisfied. Then approximately

$$\frac{\dot{v}}{v_0} = 1 + j\,\frac{\omega\,\mu\,\sigma_a}{4}\,r^2 \tag{2}$$

where $\dot{v}$ is complex amplitude of voltage in the receiver induced by the total vertical magnetic field,
$v_0$ amplitude of voltage induced in the receiver only by the primary (direct) magnetic field, i.e. in an entirely non-conducting space,
$\omega$ angular frequency of current $I$ in the transmitter dipole,
$r$ transmitter-receiver separation,
$\mu = \mu_0 = 4\pi \,.\, 10^{-7}\ H/m$ permeability of the medium,
and $\sigma_a$ apparent conductivity for a horizontally layered conducting half-space (Fig. 1)

$$\sigma_a = \sum_{i=1}^{n} \sigma_i\, Q_i \tag{3}$$

Coefficients $Q_i$ are called geometric factors (for the vertical component of the magnetic field) as they only depend on the thickness of individual layers $h_i$ and on the distance $r$ between the dipoles. They are given (Kaufmann-Keller 1983) by equations

$$Q_1 = 1 - R(\tau_1)$$

$$Q_i = R(\tau_{i-1}) - R(\tau_i) \tag{4}$$

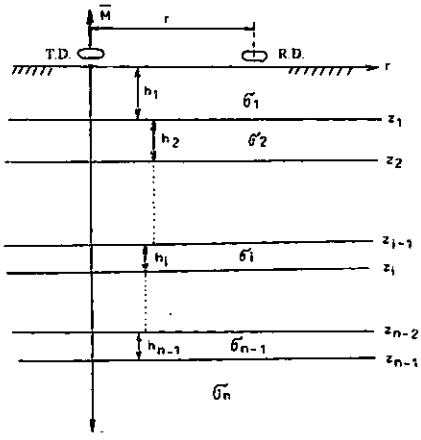


1. Vertical magnetic dipoles over a horizontally layered half-space.

for $i = 2, 3, 4 \ldots\ldots n-1$, $Q_n = R(\tau_{n-1})$
where the function $R(\tau_i)$ for vertical dipole array

$$R(\tau_i) = R_v(\tau_i) = \frac{1}{\sqrt{4\tau_i^2 + 1}} \tag{5}$$

where $\tau_i = z_i/r$ normalized depth level,
$z_i = h_1 + h_2 + \ldots\ldots h_i$ depth of the foot of $i$-th layer.

From equation (2) follows

$$\frac{\dot{v} - v_0}{v_0} = \frac{\Delta \dot{v}}{v_0} = \frac{\dot{H}_z^s}{H_z^0} = j \frac{\omega \mu \sigma_a}{4} r^2 = j \frac{H_z^s}{H_z^0}$$

i.e.

$$\sigma_a = \frac{4}{\omega \mu r^2} \frac{H_z^s}{H_z^0} = \frac{4}{\omega \mu r^2} \frac{|\Delta \dot{v}|}{v_0} \tag{6}$$

where $\dot{H}_z^s = j \frac{\omega \mu M}{16 \pi r} \sum_{i=1}^{n} \sigma_i Q_i$ (7)

is the complex amplitude of the vertical component of the secondary magnetic field in the receiver induced by eddy curents in a layered conducting half-space

$$H_z^0 = \frac{M}{4 \pi r^3} \tag{8}$$

is the amplitude of the vertical component of the primary magnetic field in the receiver induced by current in the transmitter only,

The secondary component of the magnetic field carries information on apparent conductivity. In regard to the primary component (current in the dipole) it is shifted in phase by $\pi/2$ and it is directly proportional to apparent conductivity. That is the principle of measurement of apparent conductivity with magnetic dipoles in the near field (induction conductometers). Induction conductometers are e.g. EM-31, EM-38, M-34 of Geonics Ltd., Canada and DIKO of Geofyzika Brno, Czechoslovakia. Their form depends on the required depth range. These devices facilitate geoelectric measurements at shallow depths in electromagnetic profiling and in some cases in electromagnetic sounding.

The input signal voltage $\Delta \dot{v}$ as well as the measured apparent conductivity (or vertical component of the secondary magnetic field $\dot{H}_z^s$) are given by the sum of $n$-terms (eqs. 3,6 and 7). Each term of the sum corresponds to a layer and is defined by its geometric factors and conductivity. We may afford this simplification because eddy currents in individual elementary horizontal layers of a conducting half-space are independent. The magnetic field of eddy currents in the surrounding medium, with small induction number, can be neglected. A change of conductivity in one horizontal layer will only cause a change of current in the layer and will affect neither the geometry of current lines, nor current densities in other layers. Therefore, the measured apparent conductivity is given by the sum of independent contributions of individual layers on the assumption that each contribution is dependent on the depth of the respective layer, its thickness and conductivity.

As it follows from eqs. (4), (7) or (3), the function $R$ ($\tau_i$) denotes a relative independent contribution to the secondary magnetic field (or measured apparent conductivity) of the medium as a whole under the normalized level $\tau_i$. Its derivative then determines the dependence of the relative contribution of a unit layer at the normalized depth $\tau$, which for vertical magnetic dipoles is

$$F_v(\tau) = \frac{4\tau}{\left[4\tau^2 + 1\right]^{\frac{3}{2}}} \tag{9}$$

Relationships analogous to eqs. (5) and (9), characterizing relative independent contributions, can be written for horizontal magnetic dipoles (coplanar):

$$R_H(\tau_i) = \sqrt{4\tau_i^2 + 1} - 2\tau_i \tag{10}$$

$$F_H(\tau) = 2 - \frac{4\tau}{\sqrt{4\tau^2 + 1}} \tag{11}$$

The above simplifications following from the condition of the so called "small induction number" considerably simplify solution of the direct problem, in this case calculation of apparent conductivity of the studied medium (particularly a horizontally layered half-space) as well as solution of the inverse problem in some simple cases.

## Detectability of horizontal sheets

Functions $F_V(\tau)$ and $F_H(\tau)$ illustrated in Fig. 2 demonstrate that the depth of the layer affects each type of dipole array in different way. Functions $R_V(\tau_i)$ and $R_H(\tau_i)$ which are used for a simple calculation of apparent conductivity of a horizontally layered medium are illustrated in Fig. 3. The rather simple analytical representation of these curves greatly simplifies solution of many practical problems, e.g. the problem of detectability of horizontally layered conducting or non-conducting sheets.

Fig. 4 presents a model of this problem including assumed profiles of apparent conductivity for conducting and non-conducting bodies exhibiting rotational symmetry. Horizontal dimensions of sheet $l$ with thickness $d$ and depth $h$ are considered sufficiently large compared with the distance between dipoles, i.e. $l >> r$. The maximum apparent conductivity $\sigma_{aMAX}$ at $\sigma_2 > \sigma_1$ (conducting body) and the minimum apparent

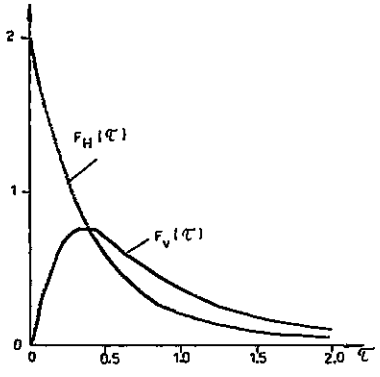


2. Dependence of the relative response to the secondary magnetic field of a unit layer on its normalized depth for vertical $F_V(\tau)$ and horizontal $F_H(\tau)$ magnetic dipoles.

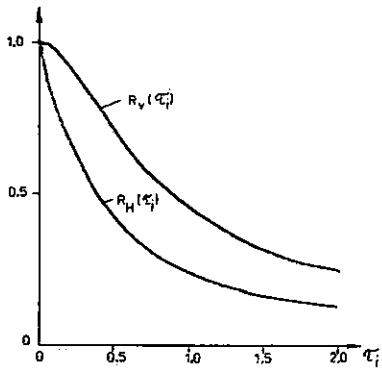


3. Relative contribution to the secondary magnetic field from below to normalized depth level $\tau_i$ for vertical $R_v(\tau_i)$ and horizontal $R_H(\tau_i)$ magnetic dipoles.

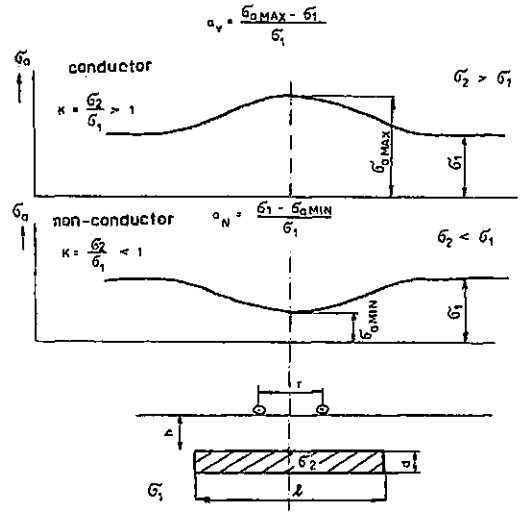


4. Model for specification of conditions for detecting a horizontally layered sheet.

conductivity $\sigma_{aMIN}$ at $\sigma_2 < \sigma_1$ (non-conducting body) will obviously appear above the centre of the body (Fig. 4).
Let us denote

$$\frac{\sigma_2}{\sigma_1} = \frac{\rho_1}{\rho_2} = k \qquad \text{conductivity contrast}$$

$$H = \frac{h}{r} \qquad \text{normalized depth of the sheet}$$

$$\Delta = \frac{d}{r} \qquad \text{normalized thickness of the sheet} \quad (12)$$

The magnitudes of conductivity anomalies (amplitudes of anomalies) are defined by

$$a_v = \frac{\sigma_{aMAX} - \sigma_1}{\sigma_1} \quad (13)$$

for a conducting body (positive anomaly)

$$a_N = \frac{\sigma_1 - \sigma_{aMIN}}{\sigma_1} \quad (14)$$

for a non-conducting body (negative anomaly).

The conditions of detectability will be characterized by the dependence of the normal-

ized thickness of the sheet on its normalized depth for induction of a conducting anomaly of the fixed magnitude $a_v(a_N)$ at a given conductivity contrast $k$, i.e.

$$\Delta = f(H) \tag{15}$$

for parameters $a_v(a_N)$, $k$.

These dependences will be established for a conducting and for a non-conducting body, at vertical and horizontal magnetic dipole array.

## Anomalies of conducting bodies

Above the centre of a sufficiently large sheet ($l >> r$) the apparent conductivity will presumably be the same as over a half-space formed by three layers with conductivities $\sigma_1$ and $\sigma_2$, and $\sigma_1$ the thickness of the middle layer $d$. Then the maximum apparent conductivity, regarding eqs. (3) and (4), is

$$\sigma_{aMAX} = \sigma_1 [1 - R(H)] + \sigma_2 [R(H) - R(H+\Delta)] + \sigma_1 R(H+\Delta)$$

Reducing it, with regard to (13), we get

$$R(H) - R(H+\Delta) = \frac{a_v}{k-1} = v \tag{16}$$

for $k > 1$.

### *A/ Vertical magnetic dipoles*

From eqs. (16) and (5) it follows that

$$v = R_v(H) - R_v(H+\Delta) = \frac{1}{\sqrt{4H^2+1}} - \frac{1}{\sqrt{4(H+\Delta)^2+1}}$$

Hence

$$\Delta = -H + \frac{1}{2} \sqrt{\frac{4H^2+1}{\left[1 - \frac{a_v}{k-1}\sqrt{4H^2+1}\right]^2} - 1} \tag{17}$$

The limits of changes of argument $H$ follow from the inequations $\Delta > 0$

$$1 > \frac{a_v}{k-1}\sqrt{4H^2+1}$$

hence

$$H \leq \frac{1}{2}\sqrt{\left(\frac{k-1}{a_v}\right)^2 - 1} = H_{MAX} \tag{18}$$

For amplitudes of anomalies and conductivity contrasts corresponding to real conditions the obtained $H_{MAX}$ is sufficiently large and always exceeds the actual depth range of vertical magnetic dipoles.

### *B/ Horizontal magnetic dipoles*

From eqs. (16) and (10) follows

$$v = \frac{a_v}{k-1} = R_H(H) - R_H(H+\Delta) = \sqrt{4H^2+1} - 2H - \left[\sqrt{4(H+\Delta)^2+1} - 2(H+\Delta)\right]$$

hence

$$\Delta = \frac{\left(\frac{a_v}{k-1}\right)^2 - 2\frac{a_v}{k-1}\sqrt{4H^2+1}}{4\left[2H + \frac{a_v}{k-1} - \sqrt{4H^2+1}\right]} \tag{19}$$

To satisfy the condition $\Delta > 0$

$$\left(\frac{a_v}{k-1}\right)^2 < 2\frac{a_v}{k-1}\sqrt{4H^2+1} \quad , 2H + \frac{a_v}{k-1} < \sqrt{4H^2+1}$$

must be true, or inverse inequations, which will never be satisfied for the considered magnitudes of anomalies and conductivity contrasts. Then

$$H < \frac{1 - \left(\frac{a_v}{k-1}\right)^2}{4\frac{a_v}{k-1}} = H_{MAX} \tag{20}$$

In this way limited depths are sufficient and in almost all cases exceed the maximum depth of horizontal dipoles, which is generally half the depth of vertical dipoles.

## Anomalies of non-conducting bodies

A non-conducting sheet (if $l >> r$) induces minimum apparent conductivity (Fig. 4) above its centre. The minimum can be defined by a three-layer model. Then

$$\sigma_{a\,MIN} = \sigma_1 [1 - R(H)] + \sigma_2 [R(H) - R(H+\Delta)] + \sigma_1 R(H+\Delta)$$

Considering eq. (14)

$$R(H) - R(H+\Delta) = \frac{a_N}{1-k} = u \tag{21}$$

for $k<1$.

Equations (16) and (21) differ only by constants $u$, $v$ on their right-hand sides. Substituting $u$ for $v$ for vertical magnetic dipoles (if $k<1$), we get

$$\Delta = -H + \frac{1}{2}\sqrt{\frac{4H^2+1}{\left[1-\frac{a_N}{1-k}\sqrt{4H^2+1}\right]^2} - 1} \tag{22}$$

$$H \leq \frac{1}{2}\sqrt{\left(\frac{1-k}{a_N}\right)^2 - 1} = H_{MAX} \tag{23}$$

for $k<1$.

Similarly for horizontal magnetic dipoles

$$\Delta = \frac{\left(\frac{a_N}{1-k}\right)^2 - 2\frac{a_N}{1-k}\sqrt{4H^2+1}}{4\left[2H + \frac{a_N}{1-k} - \sqrt{4H^2+1}\right]} \tag{24}$$

$$H < \frac{1-\left(\frac{a_N}{1-k}\right)^2}{4\frac{a_N}{1-k}} = H_{MAX} \tag{25}$$

All electromagnetic methods detect conductors much better than non-conductors. It is so with our electromagnetic method for direct and contactless measurement of apparent conductivity. Let us consider two sheets with the same geometry and depths. First of them is conducting ($k > 1$), the second is non-conducting ($k < 1$). The conductivity contrast in (16) for a conducting sheet will be $k = k_V > 1$ and in (21) for a non-conducting sheet $k = k_N < 1$.

Then

$$R(H) - R(H+\Delta) = \frac{a_V}{k_V - 1} \text{ (for } k_V>1), \qquad R(H) - R(H+\Delta) = \frac{a_N}{1-k_N} \text{ (for } k_N<1).$$

The left-hand sides of the equations are equal, assuming that their thicknesses $\Delta$ and depths $H$ are the same. We shall also assume that in regard to the surrounding medium both sheets have the same, though reciprocal, conductivity contrasts, i.e. $k_V = 1/k_N > 1$.

Then

$$\frac{a_V}{k_V - 1} = \frac{a_N}{1-k_N} = \frac{a_N}{1-\frac{1}{k_V}} = \frac{k_V a_N}{k_V - 1} \tag{26}$$

i.e. $a_v = k_v \, . \, a_N$.

The conducting body induces $k_v$-times larger anomaly than the non-conducting body at the conductivity contrasts $k_v = 1/k_N > 1$ .

### Small-size sheets

The detectability problem for small bodies whose size is comparable or smaller than the distance between dipoles will be considerably more difficult to resolve as it requires use of multidimensional models. Záhora in Hašek et al. (1988) calculated the response for induction conductometers of a small cylindrical body with rotational symmetry whose axis is identical with the axis of the transmitter dipole, and discussed its detectability. Apparent resistivity over a model consisting of n rotational symmetry areas $\Omega_i$; in a conducting finite cylindrical body of the normalized height $\tau_N$ , shown in Fig. 5, approximating a non-finite conducting half-space, is given by the relationship

$$\sigma_a = \sum_{i=1}^{n} \sigma_i \, W_i$$

where $$W_i = \frac{1}{\varphi_N} \iint_{\Omega_i} g\,(\xi, \tau)\, d\xi \, d\tau \qquad (27)$$

is the geometric factor for the $i$-th area $\Omega_i$.

Then

$$g\,(\xi, \tau) = 2 \frac{\xi}{\left[\xi^2 + \tau^2\right]^{3/2}} \cdot \frac{1}{\sqrt{(1+\xi)^2 + \tau^2}} \left[ K(\nu) + \frac{\xi^2 - 1 - \tau^2}{(1-\xi)^2 + \tau^2} E(\nu) \right] \qquad (28)$$

where $K(\nu)$, $E(\nu)$ are elliptic 1st and 2nd kind integrals

$$K_{(\nu)} = \int_0^{\pi/2} \frac{d\alpha}{\sqrt{1 - \nu^2 \sin^2 \alpha}} \qquad E_{(\nu)} = \int_0^{\pi/2} \sqrt{1 - \nu^2 \sin^2 \alpha} \; d\alpha$$

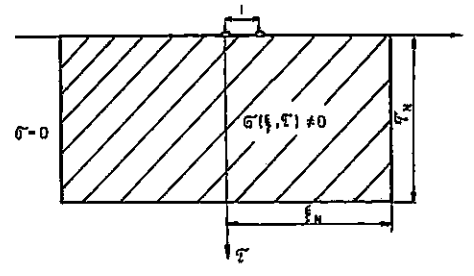


5. Model substituting the conducting half-space under the measuring dipole system.

where

$$\nu = \frac{2\sqrt{\xi}}{\sqrt{(1+\xi)^2 + \tau^2}}$$

By numerical integration it has been confirmed that for sufficiently high surface integral upper limits $\tau_N$, $\xi_N$ (over 10)

$$\varphi_N = \varphi(\xi_N, \tau_N) = \int_{\tau_L}^{\tau_N} \int_0^{\xi_N} g(\xi, \tau)\, d\tau \quad \rightarrow \pi$$

where $\xi$, $\tau$..... cylindrical coordinates (normalized variables)

$\tau_L$..... an arbitrary small positive number.

Then

$$R(\tau_i) = 1 - \frac{1}{\varphi_N} \int_{\tau_L}^{\tau_i} \int_0^{\xi_N} g(\xi, \tau)\, d\xi\, d\tau \tag{29}$$

Equation (29) for a sufficiently high $\xi_N$ is in agreement with the corresponding function for the 1-D model given by equation (5). Substituting (28) into (27), we get the geometric factor for small-size inhomogeneities having small, even negative, values. It implies poor detectability of small-size, namely non-conducting inhomogeneities. Such bodies can induce conductivity inversion, depending on their thickness and depth. It means that a conducting inhomogeneity produces a negative anomaly and a non-conducting inhomogeneity a positive anomaly. The conductivity inversion is due to a negative geometric factor. This relates to the geometry of an inhomogeneity and to the considered measuring system, as it is obvious from the distribution of the secondary magnetic field increases in the receiver dipoles due to eddy current conductors within the inhomogeneous body and in the surrounding environment. Inversion does not take place in vertical dipoles (e.g. in well-logging), and does not relate to non-linear dependence of the quadrature component of the secondary magnetic field on apparent conductivity when with increasing real conductivity of the environment over a certain limit the measured apparent conductivity decreases to negative values (as it can be observed in field measurements with induction conductometers).

In a conducting inhomogeneity the absolute value of the anomaly is

$$a_v = |a| = |W| \quad |k-1| \gg |W| \qquad \text{for } k \gg 1$$

while a non-conducting inhomogeneity induces the anomaly

$$a_N = |a| = |W| \quad |1-k| < |W|$$

The maximum absolute value of an anomaly induced by a non-conducting inhomogeneous body ($k<1$) is always limited by the corresponding geometric factor $|W|$. Anomalies due to conducting bodies are generally large.

To estimate the detectability of small horizontal sheets, we shall introduce some

simplifications. First, we shall assume a cylindrical body with the diameter $l$. It will also be assumed that the space under the dipoles, from the greater part (e.g. 90%) contributing to the secondary magnetic field, is cylindrical with the diameter $p$. Further we shall assume that all elementary parts of a particular elementary cylinder of the diameter $p$, height $dh$ and depth $h$ equally participate in the relative contribution of this elementary cylinder, with weight coefficients $\sigma_1$ or $\sigma_2$. On these rather "rough assumptions" the maximum apparent conductivity (for $p > l$) of a conducting body ($k > l$) is given by the relationship

$$\sigma_{a\,MAX} = \sigma_1 [1 - R(H) + R(H+\Delta)] + [R(H) - R(H+\Delta)] \frac{\sigma_2 \frac{\pi}{4} l^2 + \sigma_1 \frac{\pi}{4} (p^2 - l^2)}{\frac{\pi}{4} p^2} \tag{30}$$

and its minimum value for a non-conducting body ($k < 1$) is given by the same relationship when $\sigma_{a\,MAX}$ on the left-hand side is substituted by $\sigma_{a\,MIN}$
Reducing (30), we get

$$R(H) - R(H+\Delta) = v_p \qquad \text{for } k > 1 \tag{31}$$

$$\text{where } v_p = \frac{a_V m^2}{k-1} = m^2 v \tag{32}$$

$m = p/l$ and

$$R(H) - R(H+\Delta) = u_p \qquad \text{for } k < 1 \tag{33}$$

$$\text{where } u_p = \frac{a_N m^2}{1-k} = m^2 u. \tag{34}$$

Equations (31), (16) and (33), (21) characterizing anomalies of conducting and non-conducting bodies differ by constants $v$, $v_p$, $u$, $u_p$ only. Equations for "infinite" bodies can therefore be used for estimating the detectability of small bodies by substituting $v_p$ for $v$ and $u_p$ for $u$.

## Detectability curves

The detectability curves defined by eqs. (17), (19), (22) and (24), and by corresponding equations for $m>1$ were calculated with the HP 9845A computer for conducting and non-conducting bodies and for both dipole arrays for large ranges of anomaly amplitudes, conductivity contrasts and coefficients $m$. Some of the curves are presented in Figs. 6 to 24.

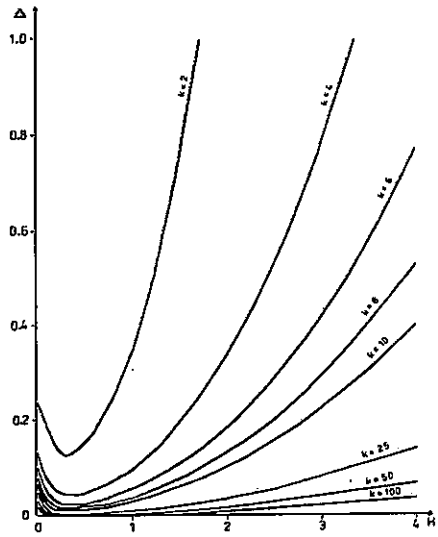


6. Dependence of the normalized thickness of a conducting body on its normalized depth for anomaly $a = 0.1$, $m = 1$ and conductivity contrasts $k = 2$, 4, 6, 8, 10, 25, 50, 100. Vertical magnetic dipoles.

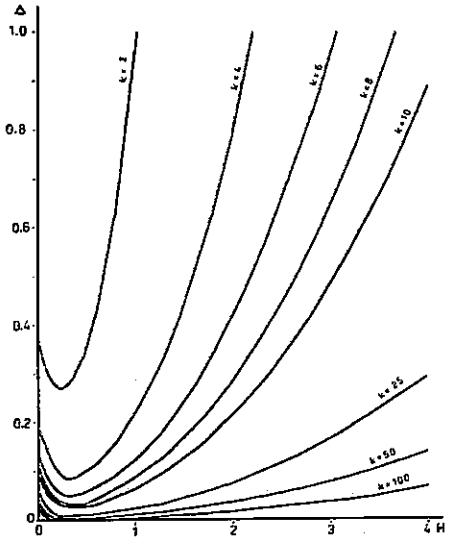


7. Dependence of the normalized thickness of a conducting body on its normalized depth for anomaly $a = 0.2$, $m = 1$ and conductivity contrasts $k = 2$, 4, 6, 8, 10, 25, 50, 100. Vertical magnetic dipoles.

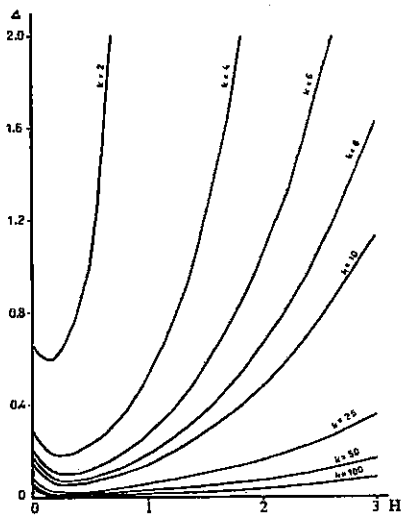


8. Dependence of the normalized thickness of a conducting body on its normalized depth for anomaly $a = 0.4$, $m = 1$ and conductivity contrasts $k = 2$, 4, 6, 8, 10, 25, 50, 100. Vertical magnetic dipoles.

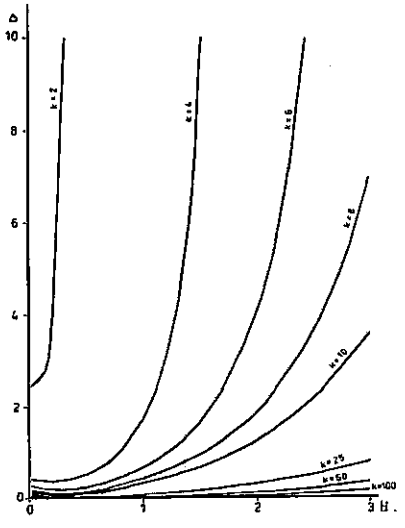


9. Dependence of the normalized thickness of a conducting body on its normalized depth for anomaly $a = 0.8$, $m = 1$ and conductivity contrasts $k = 2$, 4, 6, 8, 10, 25, 50, 100. Vertical magnetic dipoles.

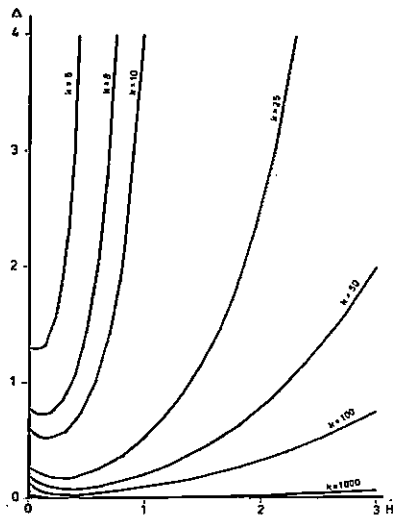


10. Dependence of the normalized thickness of a conducting body on its normalized depth for anomaly $a = 0.2$, $m = 4$ and conductivity contrasts $k = 6$, 8, 10, 25, 50, 100, 1000. Vertical magnetic dipoles.

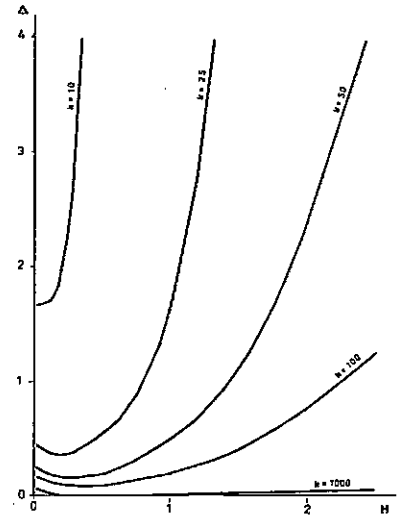


Fig. 11. Dependence of the normalized thickness of a conducting body on its normalized depth for anomaly $a = 0.4$, $m = 4$ and conductivity contrasts $k = 10$, 25, 50, 100, 1000. Vertical magnetic dipoles.

The coefficient $m$ characterizes the horizontal dimension of a body exhibiting rotational symmetry. It is $m = 1$ for $l >> r$. Greater values of $m$ correspond to small bodies whose horizontal dimension is comparable or smaller than the distance between coils. Figures 6 to 11 show the detectability curves for conducting bodies at vertical dipole array, amplitudes $a_V = 0.1$, 0.2, 0.4, 0.8 and a large range of conductivity contrasts. Two values of parameter $m$ are taken for comparison – 1 and 4.

Figs. 12 and 13 demonstrate the considerable influence of amplitude and parameter m on detectability curves if $k = 10$.

For horizontal dipoles and conducting bodies similar curves are drawn in figs. 14, 15, 16 and 17 for $m = 1$, 2, 5, amplitudes 0.2 and 0.6, and for the corresponding range of conductivity contrasts. Detectability curves for non-conducting bodies for both dipole configurations for amplitudes $a_N = 0.05$, 0.1 and 0.2, coefficients $m = 1{,}2$ and conductivity contrasts 1/2, 1/4, 1/6, 1/10, 1/50, $10^{-6}$ are in Figs. 18 to 24.

The dependence on amplitude and coefficient $m$ can be observed on all curves, see Figs. 12 and 13, and in the case of conducting bodies also on the conductivity contrast $k$. For instance, with vertical magnetic dipoles at $m = 1$, $k_N = 1/50$ a large negative anomaly $a_N = 0.2$ over a nonconducting sheet at the relative depth $H = 1$ can be created if the relative thickness of the body $\Delta = 1$, for $a_N = 0.1$ over a sheet at the same depth the thickness $\Delta = 0.36$ (i.e. 2.8 times smaller) and for $a_N = 0.05$ the thickness must be only $\Delta = 0.16$ (i.e. 6.3 times smaller). All curves confirm that it is much easier to detect conducting rather than non-conducting bodies. For instance, in the case of vertical

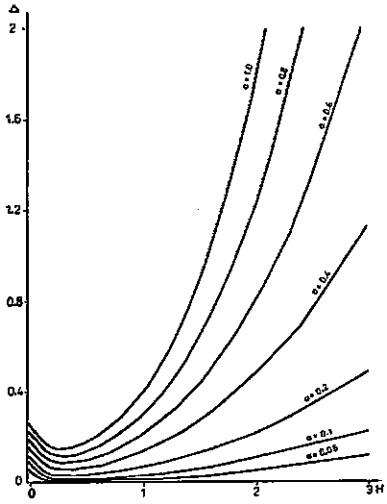

12. Dependence of the normalized thickness of a conducting sheet on its normalized depth for conductivity contrast $k = 10$, $m = 1$ and anomalies $a = 0.05, 0.1, 0.2, 0.4, 0.6, 0.8, 1$. Vertical magnetic dipoles.

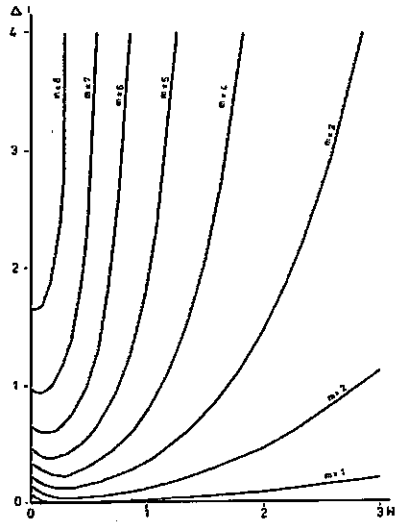

13. Dependence of the normalized thickness of a conducting sheet on its normalized depth for anomaly $a = 0.1$ ,conductivity contrast $k = 10$ and $m = 1, 2, 3, 4, 5, 6, 7, 8$. Vertical magnetic dipoles.

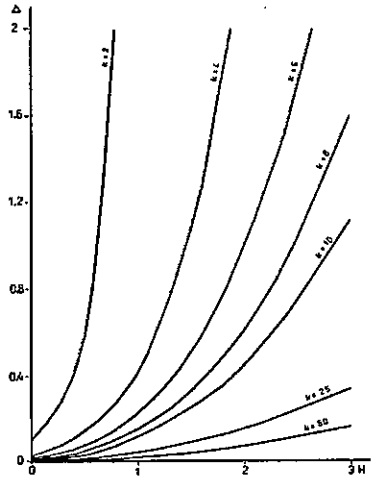

14. Dependence of the normalized thickness of a conducting body on its normalized depth for anomaly $a = 0.2$, $m = 1$ and conductivity contrasts $k = 2, 4, 6, 8, 10, 25, 50$. Horizontal magnetic dipoles.

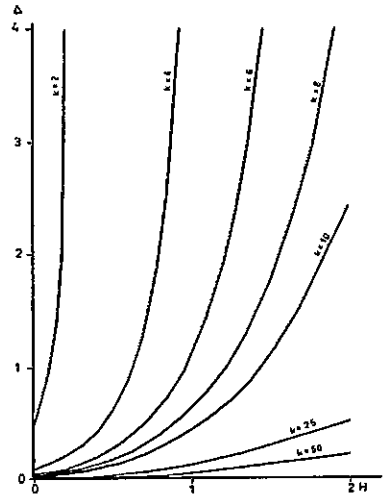

15. Dependence of the normalized thickness of a conducting body on its normalized depth for anomaly $a = 0.6$, $m = 1$ and conductivity contrasts $k = 2, 4, 6, 8, 10, 25, 50$. Horizontal magnetic dipoles.

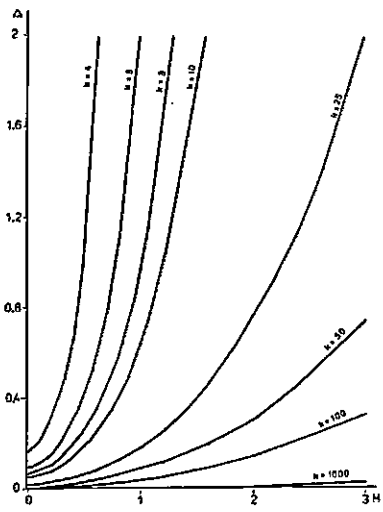


16. Dependence of the normalized thickness of a conducting sheet on its normalized depth for anomaly $a = 0.2$, $m = 2$ and conductivity contrasts $k = 4$, 6, 8, 10, 25, 50, 100, 1000. Horizontal magnetic dipoles.

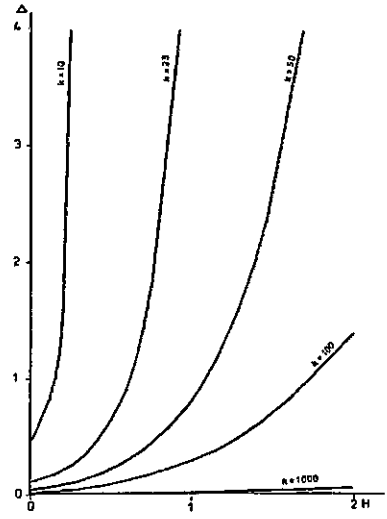


17. Dependence of the normalized thickness of a conducting sheet on its normalized depth for anomaly $a = 0.2$, $m = 5$ and conductivity contrasts $k = 10$, 25, 50,100, 1000. Horizontal magnetic dipoles.

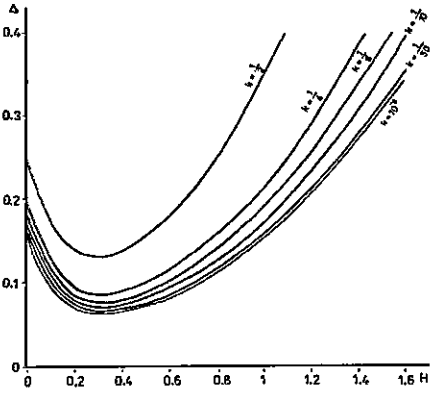


18. Dependence of the normalized thickness of a non-conducting sheet on its normalized depth for anomaly $a = 0.05$, $m = 1$ and conductivity contrasts $k = 1/2$, 1/4, 1/6, 1/10, 1/50, $10^{-6}$. Vertical magnetic dipoles.

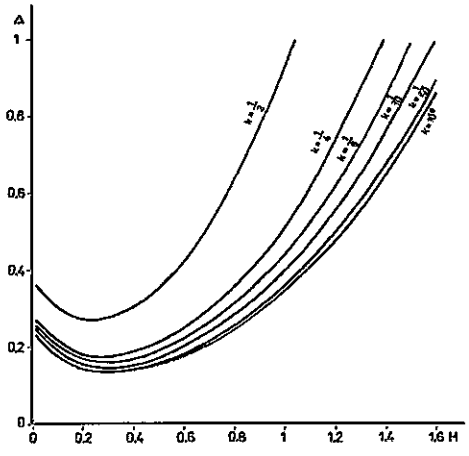


19. Dependence of the normalized thickness of a non-conducting sheet on its normalized depth for anomaly $a = 0.1$, $m = 1$ and conductivity contrasts $k = 1/2$, 1/4, 1/6, 1/10, 1/50, $10^{-6}$. Vertical magnetic dipoles.

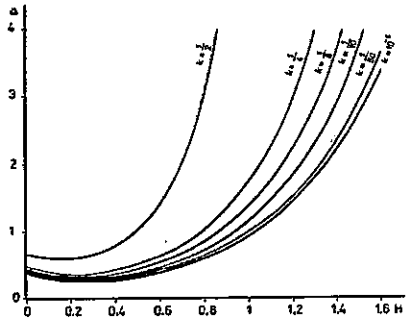

20. Dependence of the normalized thickness of a non-conducting sheet on its normalized depth for anomaly $a = 0.2$, $m = 1$ and conductivity contrasts $k = 1/2, 1/4, 1/6, 1/10, 1/50, 10^{-6}$. Vertical magnetic dipoles.

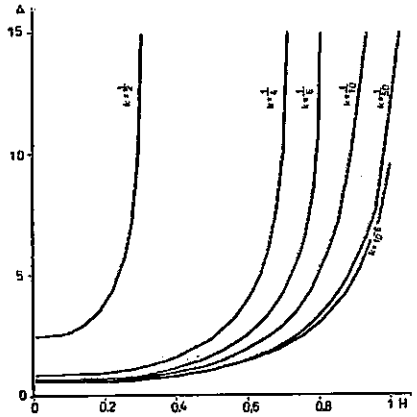

21. Dependence of the normalized thickness of a non-conducting sheet on its normalized depth for anomaly $a = 0.1$, $m = 2$ and conductivity contrasts $k = 1/2, 1/4, 1/6, 1/10, 1/50, 10^{-6}$. Vertical magnetic dipoles.

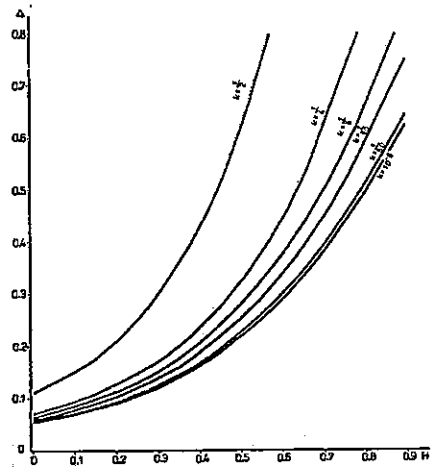

22. Dependence of the normalized thickness of a non-conducting sheet on its normalized depth for anomaly $a = 0.1$, $m = 1$ and conductivity contrasts $k = 1/2, 1/4, 1/6, 1/10, 1/50, 10^{-6}$. Horizontal magnetic dipoles.

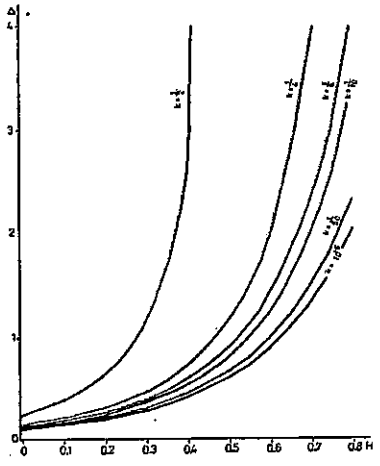

23. Dependence of the normalized thickness of a non-conducting sheet on its normalized depth for anomaly $a = 0.2$, $m = 1$ and conductivity contrasts $k = 1/2, 1/4, 1/6, 1/10, 1/50, 10^{-6}$. Horizontal magnetic dipoles.

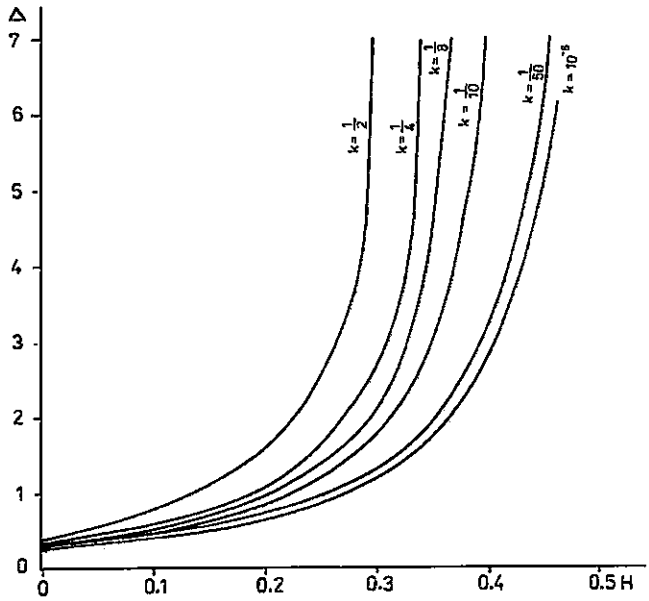


24. Dependence of the normalized thickness of a non-conducting sheet on its normalized depth for anomaly $a = 0.1$, $m = 2$ and conductivity contrasts $k = 1/2, 1/4, 1/6, 1/10, 1/50, 10^{-6}$. Horizontal magnetic dipoles.

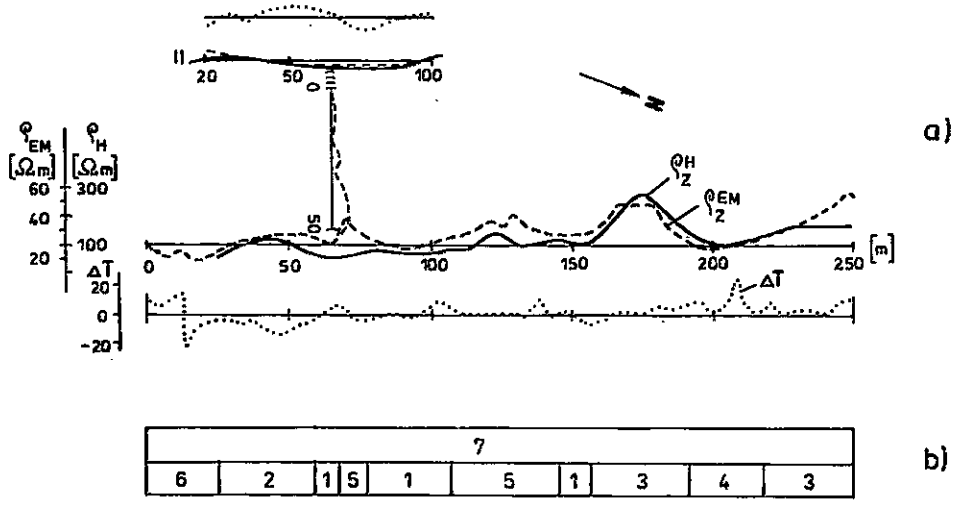


25. Resistivities distribution in Milovice, district Břeclav. a) map of resistivity lines, b) subsurface geological section; 1 – Tertiary clay, 2 – Tertiary gravel, 3 – Tertiary clastics, 4 – turbid matter, 5 – erosion scar, 6 – embankment, 7 – loess.

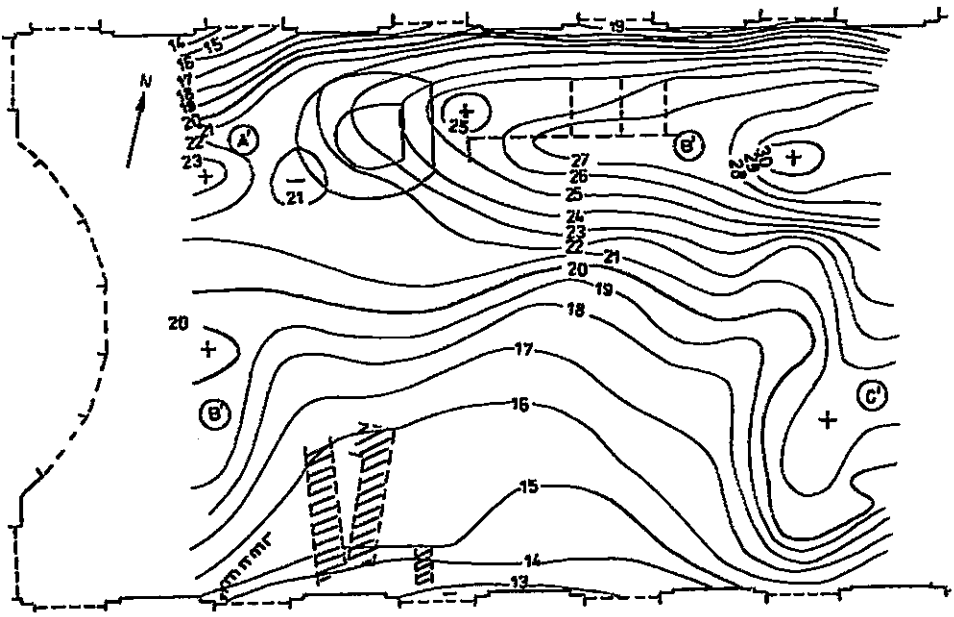


26. Map of $\rho_z^{EM}$ contours according to measurement by the DIKO induction conductometer in Slavkov, district Brno-venkov.

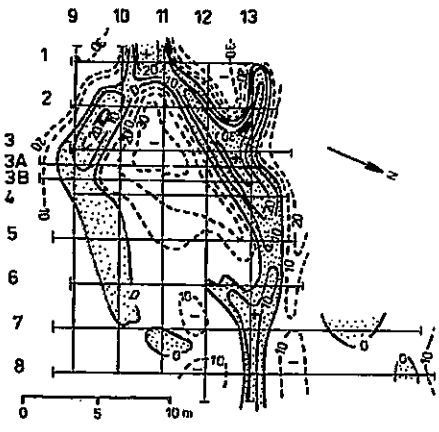


27. Map of $\rho_Z^{EM}$ contours according to measurement in Předklášteří near Tišnov, district Brno-venkov.

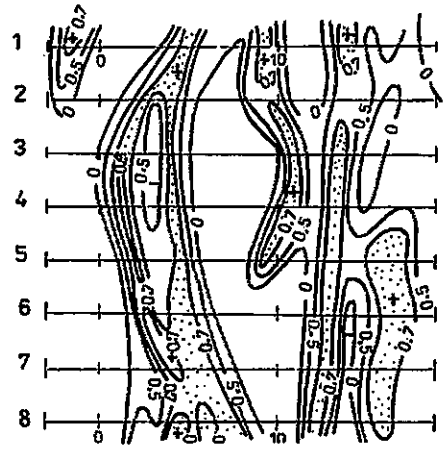


28. Map of mutual correlation coefficient according to measurement in Předklášteří near Tišnov, district Brno-venkov.

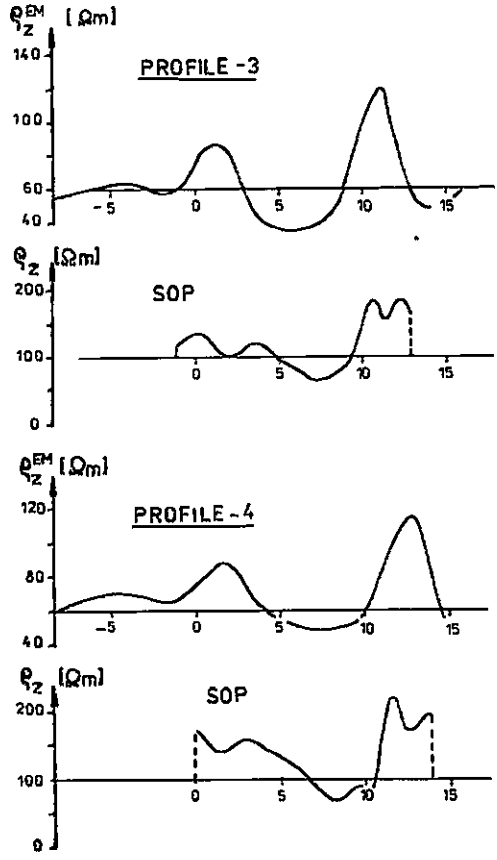


29. Comparison of profile curves $\rho_{Z(OP)}$ and $\rho_Z^{EM}$ according to measurement in Předklášteří near Tišnov, district Brno-venkov.

magnetic dipoles with $m = 1$, a positive anomaly $a_V = 0.2$ of a conducting body at the relative depth $H = 1$, conductivity contrast $k = 50$ will be induced if the relative thickness $\Delta = 0.0115$, at the contrast $k = 10$ the relative thickness $\Delta = 0.065$ (i.e. 5.6 larger). However, for a negative anomaly $a_N$=0.2 over a non-conducting body with $k = 1/50$ the thickness must be $\Delta = 1$, if $k = 1/10$ the thickness $\Delta = 1.17$. In the case of non-conducting bodies the conductivity contrast $k<1/10$ affects the curves only very slightly. If the coefficient values are low, the effect can be neglected. On the contrary, in the case of conducting bodies the thickness $\Delta$ of the sheet markedly decreases with increasing conductivity contrast. For $m = 1$, i.e. for large-scale bodies, the detectability curves reflect the reality quite well. For smaller bodies, i.e. for $m > 1$ the curves offer rather a qualitative judgement on the possibilities of detection. The different curve for vertical magnetic dipoles on the one hand, and for horizontal magnetic dipoles on the

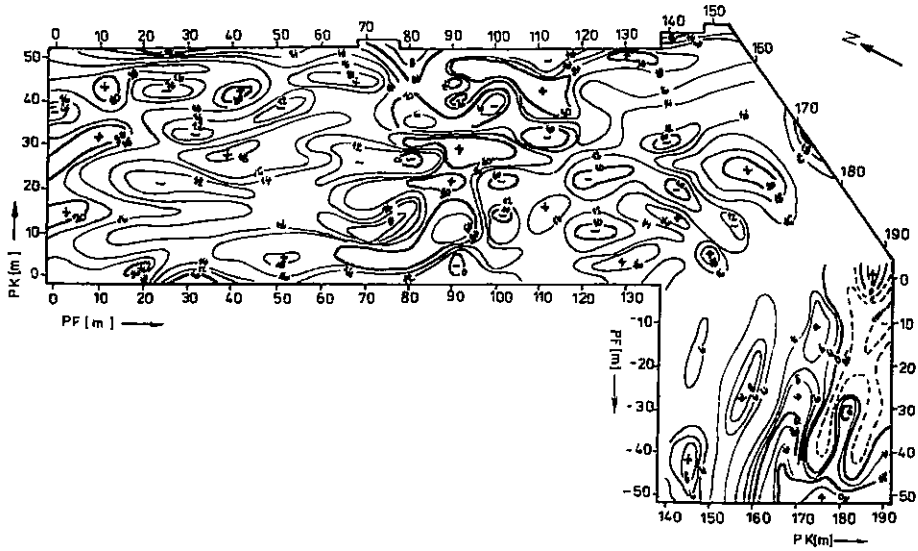


30. Map of $\rho_2^{EM}$ contours according to measurement in Rybárna, area A, Staré Město near Uherské Hradiště.

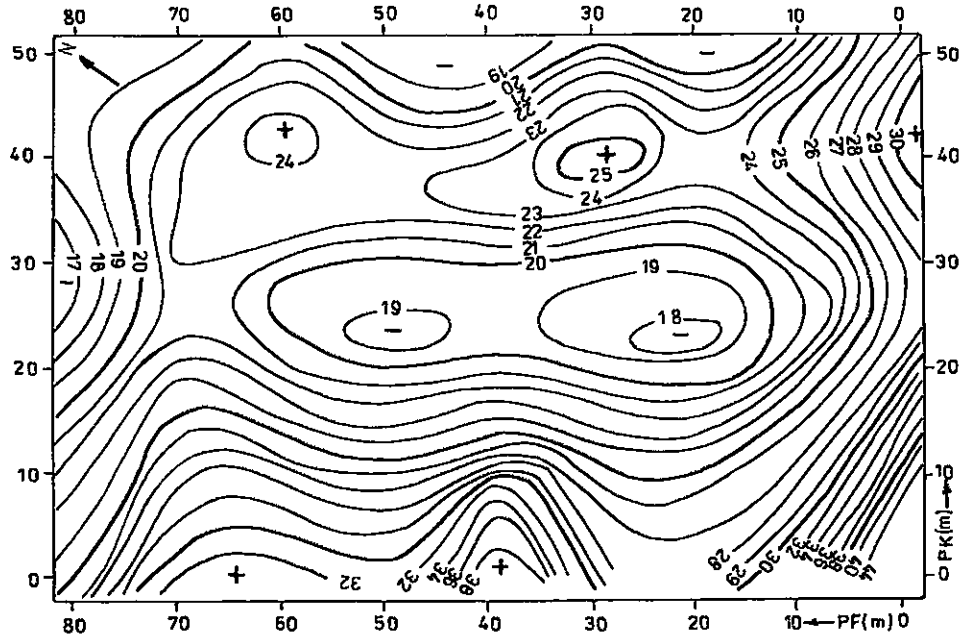


31. Map of $\rho_2^{EM}$ contours according to measurement in Rybárna, area B, Staré Město near Uherské Hradiště.

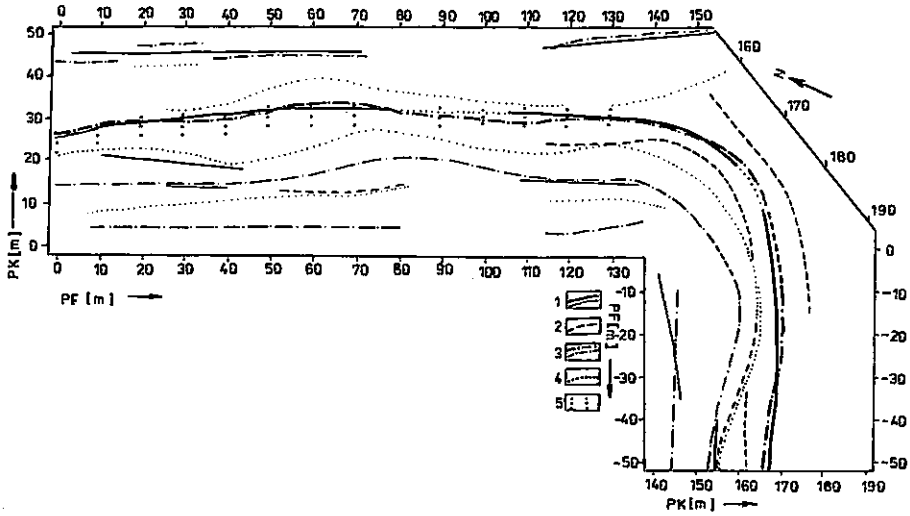


32. Comparison of geophysical measurement in Rybárna, area A, Staré Město near Uherské Hradiště. 1 – DEMP axes of non-conducting zones, 2 – DEMP axes of conducting zones, 3 – axes of positive Δ T anomalies, 4 – axes of negative Δ T anomalies, 5 – extent of morphological elevation structures.

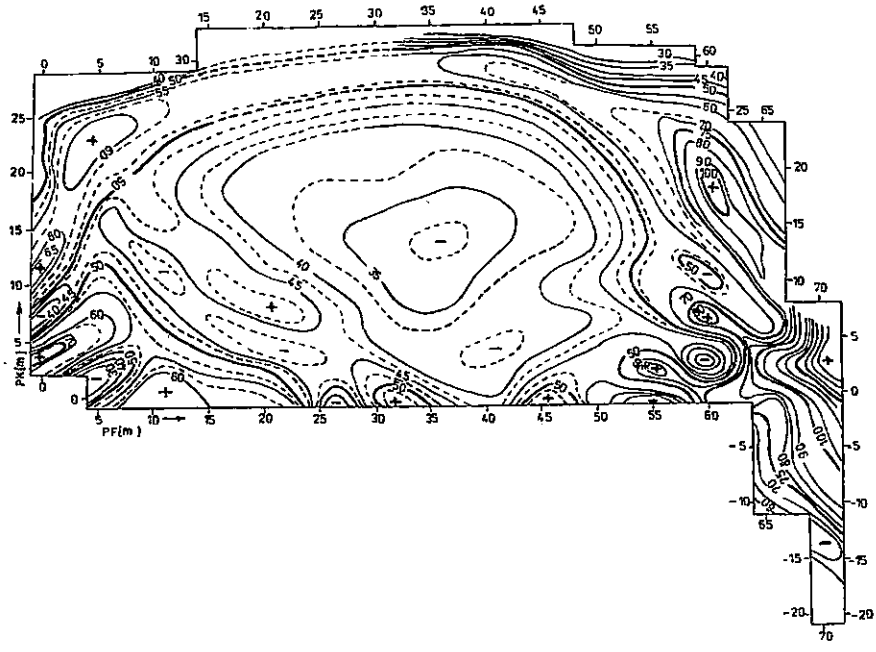


33. Map of $\rho_Z^{EM}$ contours according to measurement in Přerov, Horní náměstí ( Upper Square).

other with small $H$ (from 0 to approx. 0.5) reflect the different effects of near-surface layers on the secondary magnetic field in the receiver at respective configurations (Fig. 2).

The sharp growth of curves for non-conducting bodies ($m > 1$) suggests a very poor or zero detectability of small non-conducting bodies from certain limit depth.

## Field measurements with induction conductometers

The prototype of a device for direct and contactless apparent conductivity measurements (DIKO) has been developed in Geofyzika Brno. It is similar in principle to the EM-31 from Geonics Ltd., Canada. The prototypes are used for geophysical measurements in archaeological prospection, e.g. at Předklášteří, Staré Město, Uherské Hradiště, Bítov, Moravské Knínice, Milovice, Buchlov, Přerov-Zábřeh. Some results from reports by Hašek et al. (1988,1989) are presented here.

At the locality Milovice (district Břeclav) experimental geophysical measurements (DEMP – induction conductometer, VLF, magnetometry) were aimed at mapping of assumed erosion furrows and occurrences of Tertiary clastics in the Quaternary basement which are related with an assumed Palaeolithic settlement. A detailed geologic survey conducted along a profile running across interpreted occurrences of rocks exhibiting increased resistivity revealed two erosion furrows and a layer of Tertiary clastics (Fig. 25).

In the environs of the Slavkov u Brna castle conductivity measurements were carried out over an area of 26x20 m in a grid of 3x1 m in search for the stone foundations of the studied object. Results of measurements were processed into map of $\rho_z^{EM}$ isolines (Fig. 26) in which a number of local anomalies can be found. Increased resistivity zones (e.g. A') well correlate with magnetic data.

Resistivity profiling and conductivity measurements at Předklášteří near Tišnov were conducted to verify the assumed site of a church in the area of the museum was reconstructed. $\rho_z^{EM}$ isolines (Fig. 27) and the map of correlation coefficients (Fig. 28) indicated foundations of a small oval stone object. Results of measurements on profiles PF3 and PF4 (Fig. 29) show a good correlation between data obtained by both methods (resistivity profiling configuration was A2 M1 N2 B).

Measurements at Staré Město u Uherského Hradiště (locality "Rybárna") were aimed at defining the course of a fortification revealed by archaeological prospection.The measurements were conducted over two areas – A (200x50 m) and B (80x80 m) in a grid of 5x2 m. The results were processed into a map of $\rho_z^{EM}$ isolines (Figs. 30 and 31) and into DEMP and magnetometry correlation diagrams (Fig. 32). Increased resistivity areas revealed by conductivity measurements correspond with positive $\Delta T$ anomalies which may indicate remnants of stone masonry and a bank.

Conductivity measurements on 15 profiles (30 m each) at Horní square in Přerov were aimed at defining the course of a 10th century ditch revealed by archaeologists in the vicinity of profile 15, station 25 m. The map of $\rho_z^{EM}$ isolines (Fig. 33) and comparison with archaeological findings showed that the fortification is indicated by increased

apparent resistivities mainly in the northern part of the measured area, i.e. around 20–30 m. Decreased $\rho_2^{EM}$ values indicated a filled in fountain.

## Conclusions

If the condition of small induction number (or a near field) is satisfied, there is almost linear dependence of the secondary component of the magnetic field induced by eddy currents on apparent conductivity of a conducting half-space. The measured component of the secondary magnetic field in the receiver is shifted in phase by $\pi/2$ in regard to the primary magnetic field. Devices based on this principle (so called induction conductometers) enhance geoelectric investigations at small depths particularly in areas affected by human activity. They are applied in electromagnetic profiling, partly also in sounding to solve many practical tasks.

The present article concentrates on detection of horizontal conducting and non-conducting sheets at depth, using vertical and horizontal magnetic dipoles. The relatively easy handling of the task is due to the simple analytical representation of the relative contributions of elementary horizontal layers to the total apparent conductivity. It is conditioned by mutual independence of eddy currents in individual horizontal layers of the near field. The detectability curves were calculated using a one-dimensional model, which is suitable for sufficiently large horizontal bodies (i.e. for $l >> r$). To calculate the detectability of smaller bodies whose dimensions are comparable or less than the separation of dipoles, a multidimensional model is required. In the present article, simplified assumptions were used for detectability estimation.

Positive anomalies induced by conducting bodies prevail (they are $k$-times larger) over negative anomalies induced by non-conducting bodies. The calculated detectability curves show dependence on amplitude, and for conducting bodies on conductivity contrast. In the case of non-conducting bodies the influence of contrast $k < 1/10$ on the curves is very little. For $m = 1$ when horizontal dimensions of the body many times exceed the distance between dipoles, the detectability curves reflect reality quite well. For small bodies ($m > 1$) the curves, with regard to simplifying starting arguments, provide rather a qualitative idea about the detectability and testify to the very poor chance of detecting smaller non-conducting bodies by means of this method.

Field measurements with the developed induction conductometer prototypes confirm the positive features of the method when used at small depths. It is also obvious from the presented examples of measurements by means of induction conductometers at archaeological sites.

*K tisku doporučil J.Chyba*
*Přeložila D. Maliková*

## References

Kaufmann, A. A. - Keller, G. V. (1983): Frequency and transient soundings. – Elsevier. Amsterdam.
Záhora, R. in Hašek, V. et al. (1988): Geofyzikální příprava těžby hnědého uhlí. – MS Geofyzika, a.s. Brno.

Záhora, R. (1989): Využitelnost přímého bezkontaktního měření zdánlivé vodivosti pro účely archeologické prospekce. Sbor. Geofyzika v archeologii a moderní metody terénního výzkumu a dokumentace. – MS Geofyzika, a.s. Brno.

Hašek, V. - Měřínský, Z. (1989): IRB při archeologickém výzkumu a archeogeofyzikálním průzkumu na Moravě v letech 1986–1988. Sbor. Geofyzika v archeologii a moderní metody terénního výzkumu a dokumentace. – MS Geofyzika, a.s. Brno.

Hašek, V. et al. (1989): Geofyzikální příprava terénního archeologického výzkumu. Etapa 1989. – MS Geofyzika, a.s. Brno.

# Detekovatelnost horizontálních deskovitých těles pomocí elektromagnetických konduktometrů

*(Resumé anglického textu)*

Richard Záhora

Předloženo 11. dubna 1990

Příspěvek pojednává o elektromagnetické metodě s malým indukčním číslem, kdy hloubka vniku (skinu) značně převyšuje vzdálenost mezi vysílacím a přijímacím dipólem. Tato metoda realizovaná magnetickými dipóly v blízké zóně je využívána pro bezkontaktní určování odporových vlastností hornin. Přímé a bezkontaktní měření zdánlivé vodivosti je v tomto případě podmíněno monotónní, téměř lineární závislostí sekundární složky magnetického pole, vybuzené vířivými proudy na zdánlivé vodivosti vodivého poloprostoru. Vyhodnocovaná složka sekundárního magnetického pole v místě přijímacího dipólu je navíc fázově posunuta o $\pi/2$ oproti primárnímu magnetickému poli. Aparatury, které využívají tento efekt ( tzv. indukční konduktometry ) značně zefektivňují geoelektrický průzkum malých hloubek zejména v oblastech s intenzívní lidskou činností. Využívají se při elektromagnetickém profilování a částečně i sondování, které pro mnoho praktických úloh je dostačující.Jsou to např. přístroje EM-31, EM-38,EM-34, vyráběné kanadskou firmou Geonics, Ltd. a DIKO a.s. Geofyzika Brno, jejichž provedení závisí zejména na požadovaném hloubkovém dosahu.

Hlavní pozornost článku je věnována hloubkové detekovatelnosti horizontálně uložených vodivých a nevodivých deskovitých nehomogenit při vertikálním a horizontálním uspořádání magnetických dipólů. Hloubkovou detekovatelnost definujeme závislostí normované mocnosti $\Delta$ deskovité nehomogenity na normované hloubce $H$ jejího uložení pro vytvoření vodivostní anomálie fixované velikosti $a_v$ ($a_N$ ) při daném kontrastu vodivostí $k$, tj. závislostí $\Delta = f(H)$ pro parametry $a_v$ ($a_N$ ), $k$.

Poměrně snadné řešení této úlohy vyplývá z jednoduchého analytického vyjádření relativních nezávislých příspěvků elementárních horizontálních vrstev k celkovému sekundárnímu magnetickému poli či celkové měřené zdánlivé měrné vodivosti.Tyto příspěvky jsou charakterizovány funkcemi $F_V(\tau)$ či $F_H(\tau)$ nebo $R_V(\tau)$ a $R_H(\tau)$ pro vertikální a horizontální uspořádání magnetických dipólů, které jsou znázorněny na obr. 2 a 3. Jednoduché vyjádření těchto funkcí (viz rovnice 5, 9, 10 a 11) vyplývá ze vzájemné nezávislosti vířivých proudů v jednotlivých horizontálních vrstvách blízké zóny.

Pro stanovení křivek detekovatelnosti je využit jednorozměrný model,který je oprávněný pouze pro dostatečně rozlehlé nehomogenity v horizontální rovině, tj. pro $l >> r$ (viz obr. 4). Úloha detekovatelnosti menších nehomogenit, jejichž rozměry jsou přibližně stejné jako rozestup mezi dipóly nebo menší, je podstatně složitější, neboť vyžaduje řešení vícerozměrných modelů. Pro přibližné hodnocení detekovatelnosti menších horizontálních deskovitých nehomogenit byly zavedeny značně zjednodušující předpoklady.

Křivky detekovatelnosti byly vyčísleny pro vodivé a nevodivé nehomogenity a obě

uspořádání dipolů pro značná rozmezí amplitud anomálií, vodivostních kontrastů a koeficientů $m$. Některé z těchto křivek jsou vyneseny na obr. 6–24. Koeficient $m$ charakterizuje horizontální rozlehlost nehomogenity, která je uvažována rotačně symetrická, pro $l >> r$ je $m = 1$. Větší hodnoty $m$ odpovídají menším nehomogenitám, jejichž horizontální rozměr je porovnatelný s rozestupem mezi cívkami nebo menší.

Popisovaná elektromagnetická metoda pro přímé a bezkontaktní měření zdánlivé vodivosti detekuje podle očekávání daleko výrazněji vodiče než nevodiče, jak dokumentují všechny křivky. Kladné anomálie vytvořené vodivými nehomogenitami převyšují $k$-krát amplitudy záporných anomálií nevodivých nehomogenit při jejich stejné geometrii i hloubce uložení. Všechny křivky vykazují očekávanou poměrně značnou závislost na amplitudě anomálie a koeficientu $m$ (jak je patrno z obr. 12 a 13) a u vodivých nehomogenit na poměru vodivostí $k$. U nevodivých homogenit při $k < 1/10$ poměrně málo ovlivňuje průběh všech křivek, při $k << 1/10$ je jeho vliv prakticky zanedbatelný.

Pro $m = 1$, tj. pro značně rozlehlé nehomogenity, odpovídají křivky detekovatelnosti vcelku dobře skutečným poměrům. Pro menší nehomogenity při $m>1$ poskytují příslušné křivky s ohledem na značně zjednodušené výchozí předpoklady pouze orientační údaje.

V závěru příspěvku jsou uvedeny výsledky měření s popsanou elektromagnetickou metodou při archeologickém průzkumu lokality Milovice, okr.Břeclav, zámku Slavkova u Brna, v Předklášteří u Tišnova, ve Starém Městě a v Přerově. Výsledky těchto měření potvrdily efektivnost a výhodnost této elektromagnetické metody při průzkumu malých hloubek.

### Vysvětlivky k obrázkům

1. Vertikální magnetické dipóly nad vrstevnatým poloprostorem.
2. Závislost relativního příspěvku (odezvy) k sekundárnímu magnetickému poli jednotkové vrstvy na normované hloubce jejího uložení pro vertikální $F_V(\tau)$ a horizontální $F_H(\tau)$ magnetické dipóly.
3. Relativní příspěvek k sekundárnímu magnetickému poli celého prostředí nalézajícího se pod normovanou hloubkovou úrovní $\tau_i$ pro vertikální $R_V(\tau_i)$ a horizontální $R_H(\tau_i)$ magnetické dipóly.
4. Model pro stanovení podmínek detekovatelnosti horizontálně uložené deskové nehomogenity.
5. Model nahrazující nekonečný vodivý poloprostor pod měřicím dipólovým systémem.
6. Závislost normované mocnosti vodivé deskové nehomogenity na normované hloubce jejího uložení pro anomálii $a = 0,1$, $m = 1$ a poměry vodivostí $k = 2, 4, 6, 8, 10, 25, 50, 100$. Vertikální magnetické dipóly.
7. Závislost normované mocnosti vodivé deskové nehomogenity na normované hloubce jejího uložení pro anomálii $a = 0,2$, $m = 1$ a poměry vodivostí $k = 2, 4, 6, 8, 10, 25, 50, 100$. Vertikální magnetické dipóly.
8. Závislost normované mocnosti vodivé deskové nehomogenity na normované hloubce jejího uložení pro anomálii $a = 0,4$, $m = 1$ a poměry vodivostí $k = 2, 4, 6, 8, 10, 25, 50, 100$. Vertikální magnetické dipóly.
9. Závislost normované mocnosti vodivé deskové nehomogenity na normované hloubce jejího uložení pro anomálii $a = 0,8$, $m = 1$ a poměry vodivostí $k = 2, 4, 6, 8, 10, 25, 50, 100$. Vertikální magnetické dipóly.
10. Závislost normované mocnosti vodivé deskové nehomogenity na normované hloubce jejího uložení pro anomálii $a = 0,2$, $m = 4$ a poměry vodivostí $k = 6, 8, 10, 25, 50, 100, 1000$. Vertikální magnetické dipóly.
11. Závislost normované mocnosti vodivé deskové nehomogenity na normované hloubce jejího uložení pro anomálii $a = 0,4$, $m = 4$ a poměry vodivostí $k = 10, 25, 50, 100, 1000$. Vertikální magnetické dipóly.
12. Závislost normované mocnosti vodivé deskové nehomogenity na normované hloubce jejího uložení pro poměr vodivostí $k = 10$, $m = 1$ a anomálie $a = 0,05, 0,1, 0,2, 0,4, 0,6, 0,8, 1$. Vertikální magnetické dipóly.
13. Závislost normované mocnosti vodivé deskové nehomogenity na normované hloubce jejího uložení pro anomálii $a = 0,1$, poměr vodivostí $k = 10$ a $m = 1, 2, 3, 4, 5, 6, 7, 8$. Vertikální magnetické dipóly.

14. Závislost normované mocnosti vodivé deskové nehomogenity na normované hloubce jejího uložení pro anomálii $a$ =0,2, $m$ =1 a poměry vodivostí $k$ =2, 4, 6, 8, 10, 25, 50. Horizontální magnetické dipóly.
15. Závislost normované mocnosti vodivé deskové nehomogenity na normované hloubce jejího uložení pro anomálii $a$ =0,6, $m$ =1 a poměry vodivostí $k$ =2, 4, 6, 8, 10, 25, 50. Horizontální magnetické dipóly.
16. Závislost normované mocnosti vodivé deskové nehomogenity na normované hloubce jejího uložení pro anomálii $a$ =0,2, $m$ =2 a poměry vodivostí $k$ =4, 6, 8, 10, 25, 50, 100, 1000. Horizontální magnetické dipóly.
17. Závislost normované mocnosti vodivé deskové nehomogenity na normované hloubce jejího uložení pro anomálii $a$ =0,2, $m$ =5 a poměry vodivostí $k$ =10, 25, 50, 100, 1000. Horizontální magnetické dipóly.
18. Závislost normované mocnosti nevodivé deskové nehomogenity na normované hloubce jejího uložení pro anomálii $a$ =0,05, $m$ =1 a poměry vodivostí $k$ =1/2, 1/4, 1/6, 1/10, 1/50, $10^{-6}$. Vertikální magnetické dipóly.
19. Závislost normované mocnosti nevodivé deskové nehomogenity na normované hloubce jejího uložení pro anomálii $a$ =0,1, $m$ =1 a poměry vodivostí $k$ =1/2, 1/4, 1/6, 1/10, 1/50, $10^{-6}$. Vertikální magnetické dipóly.
20. Závislost normované mocnosti nevodivé deskové nehomogenity na normované hloubce jejího uložení pro anomálii $a$ =0,2, $m$ =1 a poměry vodivostí $k$ =1/2, 1/4, 1/6, 1/10, 1/50, $10^{-6}$. Vertikální magnetické dipóly.
21. Závislost normované mocnosti nevodivé deskové nehomogenity na normované hloubce jejího uložení pro anomálii $a$ =0,1, $m$ =2 a poměry vodivostí $k$ =1/2, 1/4, 1/6, 1/10, 1/50, $10^{-6}$. Vertikální magnetické dipóly.
22. Závislost normované mocnosti nevodivé deskové nehomogenity na normované hloubce jejího uložení pro anomálii $a$ =0,1 , m = 1 a poměry vodivostí $k$ =1/2, 1/4, 1/6, 1/10, 1/50, $10^{-6}$. Horizontální magnetické dipóly.
23. Závislost normované mocnosti nevodivé deskové nehomogenity na normované hloubce jejího uložení pro anomálii $a$ =0,2, $m$ =1 a poměry vodivostí $k$ =1/2, 1/4, 1/6, 1/10, 1/50, $10^{-6}$. Horizontální magnetické dipóly.
24. Závislost normované mocnosti nevodivé deskové nehomogenity na normované hloubce jejího uložení pro anomálii $a$ =0,1, $m$ =2 a poměry vodivostí $k$ =1/2, 1/4, 1/6, 1/10, 1/50, $10^{-6}$. Horizontální magnetické dipóly.
25. Rozložení odporů v Milovicích, okr.Břeclav.
    a) mapa odporových profilů, b) podpovrchový geologický řez; 1 – terciérní jíl, 2 – terciérní štěrk, 3 – terciérní klastika, 4 – splachové sedimenty, 5 – erozní rýha, 6 – navážka, 7 – spraš.
26. Mapa izolinií $\rho_Z^{EM}$ podle měření s indukčním konduktometrem DIKO ve Slavkově u Brna.
27. Mapa izolinií $\rho_Z^{EM}$ z měření v Předklášteří u Tišnova,okr. Brno - venkov.
28. Mapa koeficientů vzájemné korelace z měření v Předklášteří u Tišnova,okr. Brno-venkov.
29. Porovnání profilových křivek $\rho_{Z\,(OP)}$ a $\rho_Z^{EM}$ z měření v Předklášteří u Tišnova,okr. Brno-venkov.
30. Mapa izolinií $\rho_Z^{EM}$ z měření v Rybárně, plocha A, Staré Město u Uherského Hradiště.
31. Mapa izolinií $\rho_Z^{EM}$ z měření v Rybárně, plocha B, Staré Město u Uherského Hradiště.
32. Korelační schéma z měření v Rybárně, plocha A, Staré Město u Uherského Hradiště.
    1 – osy nevodivých pásem z metody DEMP, 2 – osy vodivých pásem z metody DEMP, 3 – osy pozitivních anomálií $\Delta T$, 4 – osy negativních anomálií $\Delta T$, 5 – rozsah morfologických elevačních struktur.
33. Mapa izolinií $\rho_Z^{EM}$ z měření v Přerově na Horním náměstí.

**SBORNÍK GEOLOGICKÝCH VĚD**
**JOURNAL OF GEOLOGICAL SCIENCES**

**užitá geofyzika**

**applied geophysics**

**25**

Vydal Český geologický ústav
Praha 1992

Vědecký redaktor: RNDr. Karel Cidlinský, CSc.

Obálku navrhl M.Cihelka
Odpovědná redaktorka: V. Čechová
Technická redaktorka: J. Pavlíčková
Sazbu programem Ventura 4.0 provedlo vydavatelství ČGÚ,
Malostranské nám. 19, Praha 1
Tisk: Tercie, s.s r.o., V Šáreckém údolí 39, Praha 6

Vydání I. — 144 stran, 12,63 AA — 12,83 VA
Náklad 500 výtisků — 03/9— 446-421-92
ISBN 80-7075-110-X ISSN 0036-5319